Revista Virtual de Química

ISSN 1984-6835

Artigo

Ni/C-CeO_2 with Different Morphologies of CeO_2 Towards Urea Electro-Oxidation Reaction

Tanabe, N. B. M.; Barbosa, J. R.; Checca, N. R.; Rodrigues, T. S.; Silva, F. A.; Alves, O. C.; Silva, J. C. M.*

Rev. Virtual Quim., **2020**, *12* (6), 0000-0000. Data de publicação na Web: 17 de Setembro de 2020

http://rvq.sbq.org.br

Ni/C-CeO_2 com Diferentes Morfologias de CeO_2 frente a Reação de Eletro-Oxidação da Ureia

Resumo: A ureia, além de estar presente na urina humana, é produzida como fertilizante em indústrias. Dessa forma, grande quantidade desse composto é lançada diariamente em efluentes. A oxidação eletroquímica da ureia é um método promissor para remoção desse composto. Assim, neste trabalho, nanopartículas de Ni suportadas em carbono e CeO_2 com diferentes morfologias, foram sintetizadas com o intuito de estudar a influência da presença do CeO_2 no processo de eletro-oxidação de ureia. As análises de difração de raios-x (DRX) revelaram a presença das fases Ni° e $Ni(OH)_2$ e confirmaram a presença do CeO_2 e do carbono. As imagens de microscopia eletrônica de transmissão (MET) confirmaram nanofios de CeO_2 com diâmetros de 15 nm e nanopartículas de Ni com 2 nm de tamanho. A atividade catalítica dos materiais foi investigada por experimentos de voltametria cíclica (VC) e cronoamperometria (CA), nos quais foi mostrado que a presença de céria aumentou a atividade catalítica na reação de oxidação eletroquímica da ureia.

Keywords: Nanopartículas de Ni; nanofios de CeO_2; eletro-oxidação de ureia.

Abstract

Urea, in addition to being present in human urine, is produced as a fertilizer in industries. Thus, a large amount of this compound is discharged daily into effluents. The electrochemical oxidation of urea is a promising method for removing this compound. Thus, in this work, Ni nanoparticles supported on carbon and CeO_2 with different morphologies were synthesized in order to study the influence of CeO_2 in the urea electro-oxidation process. X-ray diffraction (XRD) analyzes revealed the presence of the Ni° and $Ni(OH)_2$ phases and confirmed the presence of CeO_2 and carbon. Transmission electron microscopy (TEM) images confirmed CeO_2 nanowires with diameter of 15 nm and Ni nanoparticles with 2 nm in size. The catalytic activity of the materials was investigated by cyclic voltammetry (CV) and chronoamperometry (CA) experiments, in which it was shown that the presence of ceria increased the catalytic activity in the electrochemical oxidation of urea reaction.

Palavras-chave: Ni nanoparticles; CeO_2 nanowires; urea electro-oxidation.

* Universidade Federal Fluminense, Instituto de Química, Departamento de Físico-Química, Campus do Valonguinho, CEP 24020-140, Niterói-RJ, Brazil.

juliocms@id.uff.br

DOI: 10.21577/1984-6835.20200112

Volume 12, Número 6 Novembro-Dezembro 2020

Revista Virtual de Química
ISSN 1984-6835

Ni/C-CeO_2 with Different Morphologies of CeO_2 Towards Urea Electro-Oxidation Reaction

Nássara Bárbara Mendes Tanabe,[a] Joseane Ribeiro Barbosa,[a] Noemi Raquel Checca,[b] Thenner Silva Rodrigues,[c] Felipe Anchieta Silva,[c] Odivaldo Cambraia Alves,[a] Júlio César Martins da Silva[a,*]

[a] Universidade Federal Fluminense, Instituto de Química, Departamento de Físico-Química, Campus do Valonguinho, CEP 24020-140, Niterói-RJ, Brasil.
[b] Centro Brasileiro de Pesquisas Físicas, CEP 22290-180, Rio de Janeiro-RJ, Brasil.
[c] Universidade Federal do Rio de Janeiro, Instituto Alberto Luiz Coimbra de Pós-Graduação e Pesquisa de Engenharia, CEP 21941-972, Rio de Janeiro-RJ, Brasil.

*juliocms@id.uff.br

Recebido em 25 de Junho de 2020. Aceito para publicação em 14 de Agosto de 2020.

1. Introduction

Fresh water is a scarce resource and its consumption has been gradually increasing with population growth.[1] Everyday, large amounts of wastewater containing urea are generated. Urea is an organic compound with formula H_2NCONH_2 that is produced on a large scale in industry as an agricultural fertilizer and animal feed additive.[2]

Urea is also found in domestic effluent, since it is present in human and animal urine.[3] Human urine contains around 2 to 2.5% of urea by weight[4] and, considering that an adult produces on average about 33 g urea per day,[2] it can be concluded that there is a high concentration of urea in municipal effluents.

Several environmental problems can occur from inadequate disposal of these wastewater containing urea, because it can naturally decompose into ammonia, which is toxic to aquatic organisms and then also be emitted into the atmosphere. Ammonia in the atmosphere is unstable and can be oxidized to other nitrogen

pollutants such as nitrates, nitrites and nitric oxides, and consequently can promote the formation of acid rain.[5]

Thus, the development of technologies for urea degradation is important. The electrochemical oxidation of urea from wastewater rich in this compound has attracted much attention because it is a well-controlled technique and does not produce toxic compounds to the environment, except for carbon dioxide.[2] Furthermore, this technique also presents the capacity of hydrogen generation, considered an alternative fuel. In the anode, the oxidation of urea in nitrogen and carbon dioxide occurs, while in the cathode, it occurs the reduction of water to hydrogen and hydroxyl ions.[6] These reactions (Eq. 1-3) can be observed as it follows:[7]

Anode: $CO(NH_2)_{2(aq)} + 6OH^-_{(aq)} \rightarrow N_{2(g)} + 5H_2O_{(l)} + CO_{2(g)} + 6e^-$ (1)

Cathode: $6H_2O_{(l)} + 6e^- \rightarrow 3H_{2(g)} + 6OH^-_{(aq)}$ (2)

Global: $CO(NH_2)_{2(aq)} + H_2O_{(l)} \rightarrow N_{2(g)} + CO_{2(g)} + 3H_{2(g)}$ (3)

Nickel-based catalysts are the most efficient for the electro-oxidation reaction of urea due to their good catalytic activity and, because nickel is a non-noble metal and it is low cost.[8] The electro-oxidation reactions of urea with nickel as a catalyst in alkaline medium can be expressed as follows (Eq. 4-7):[4,7]

Anode: $6Ni(OH)_{2(s)} + 6OH^-_{(aq)} \rightarrow 6NiOOH_{(s)} + 6H_2O_{(l)} + 6e^-$ (4)

$6NiOOH_{(s)} + CO(NH_2)_{2(aq)} + H_2O_{(l)} \rightarrow 6Ni(OH)_{2(s)} + CO_{2(g)} + N_{2(g)}$ (5)

Cathode: $6H_2O_{(l)} + 6e^- \rightarrow 3H_{2(g)} + 6OH^-_{(aq)}$ (6)

Global: $CO(NH_2)_{2(aq)} + H_2O_{(l)} \rightarrow CO_{2(g)} + N_{2(g)} + 3H_{2(g)}$ (7)

Nanomaterials are preferably used as catalysts due to their ability to increase electrocatalytic efficiency, large the surface area and improve reaction rates due to their excellent and unique physicochemical properties.[9]

Some factors influence the catalytic activity of a material, such as the combination of two or more elements, the addition of supports and the morphology.[10,11] That way, various strategies are adopted in different applications in electrocatalysis. For example, the preparation of catalysts with core-shell structure with the following composition SnO_2@Pt/C, Ni@Pt/C and NiSn@Pt/C[12] and catalysts with distinct compositions Pt/C, $Pt_{80}Ir_{20}$/C, $Pt_{80}W_{20}$/C, $Pt_{80}Sn_{20}$/C and $Pt_{60}Ir_{10}Sn_{30}$/C.[13]

The addition of a second metal such as cobalt (Co), manganese (Mn) and cadmium (Cd) to a nickel-based catalyst increases the catalytic activity of this metal in the process of the electro-oxidation reaction of urea.[14] Additionally, in a previous publication of our research group, it was shown that the addition of a lower amount of platinum to nickel catalysts ($Ni_{95}Pt_5$/C and $Ni_{90}Pt_{10}$/C) results in an enhancement in the catalytic activity towards urea electro-oxidation.[15] The use of supports such as carbon nanowires and graphene also promote an increase in the catalytic activity of Ni.[14] Regarding the support materials, carbon-based supports are considered appropriate for electrocatalysts, because they present good electrical conductivity and chemical resistance.[16]

Ceria (CeO_2) has a remarkable importance in several applications in catalysis, because the oxygen vacancy defects formed are quickly eliminated, providing high oxygen storage capacity.[17] In addition to this characteristic, another great importance of ceria is the presence of the pair Ce^{3+}/Ce^{4+} that allows the oxygen mobility in the crystalline structure.[18]

Therefore, the combination of the metals Ni and Ce in the preparation of catalysts for application in the process of the electro-oxidation of urea is very promising because of the oxygen storage capacity, the low cost of the system,[19] the catalytic activity of Ni and the synergistic effects of Ni and Ce. Additionally, the presence of Ce with Ni makes possible to extract higher current density from urea electro-oxidation process. Another extremely important function of ceria is to promote the oxidation of carbon monoxide (CO), generated during the oxidation of urea, which is capable of deactivating the NiOOH species responsible for promoting the electro-oxidation of urea.[8]

Morphology is also an important factor in the electrocatalytic activity of materials, because it appoints the preferential exposure of crystalline planes.[20] Cerium nanowires have the reactive planes {110} and {100} preferably exposed on their surfaces, conferring a superior catalytic activity to the CO oxidation process when compared to other morphologies.[21]

Considering the aspects described, this work had as a purpose,The synthesis characterization of nickel nanoparticles supported on Vulcan® carbon and a physical mixture of Vulcan® carbon (80%) and CeO_2 (20%) with different morphologies

(nanowires and approximately spherical particles) to be applied as catalysts in the process of urea electro-oxidation.

2. Material and Methods

2.1. Chemicals

Ethanol (99.5% Synth®), nitrogen, sodium borohydride (99% Sigma-Aldrich®), nickel nitrate hexahydrate (Sigma-Aldrich®), Vulcan® carbon, Nafion® 5%, isopropyl alcohol (99.8% Synth®), deionised water, cerium nitrate hexahydrate (99.5% Sigma-Aldrich®) and sodium hydroxide (99% Sigma-Aldrich®) were analytical grade and used without further purification. CeO_2 powder, (99.995% Sigma-Aldrich®) was used as commercial material.

2.2. Synthesis of cerium oxide nanowires

The synthesis of CeO_2 nanowires was performed based on the hydrothermal method.[22] For this purpose, 19.6 g of NaOH were dissolved in 35 mL of deionized water and, later, the solution was transferred to a stainless-steel autoclave covered with Teflon®. Soon after, 6.95 g of $Ce(NO_3)_3.6H_2O$ were dissolved in 5 mL of deionized water, followed by the gradual transfer of the solution to the autoclave. The autoclave was heated for 24 h at 110 °C and then cooled to room temperature. The products were collected by centrifugation. Three washes with ethanol and three washes with water were performed. Finally, the prepared materials were dried at 110 °C for 6 h.[23]

2.3. Synthesis of nickel nanoparticles

In the synthesis of Ni/C nanoparticles, 200 mg of catalyst were prepared, with a weight composition of 20% nickel and 80% carbon. In this process, 0.205 g $Ni(NO_3)_2.6H_2O$ was dispersed in 100 mL of ethanol under constant agitation at room temperature (about 22 °C). The solution had a pH value equivalent to 5. Subsequently, 0.1596 g of carbon was added to this solution. Then, N_2 was purged for 30 minutes. After that, 0.1334 g of $NaBH_4$, a mass necessary for a molar ratio of 5:1 of $NaBH_4$:Ni, was weighed. The solution was dissolved in 5 mL of cold deionized water, followed by a transfer to the nickel solution. The solution was kept under agitation for another 15 minutes. Soon after, to obtain the separation of the nanoparticles, the dispersion was centrifuged, so that 4 washes were made, two with deionized water and two with ethanol. Finally, the resulting material was dried for 12 h in the oven at 70 °C.

For the synthesis of the nanowire and commercial Ni/C-CeO_2 nanoparticles, 200 mg of catalyst were prepared, with compositions of 20% by weight of nickel, 64% of carbon and 16% of cerium oxide. The same procedure presented previously was performed, changing only the values of the masses. In Table 1 below, they are shown the values of the masses used in the syntheses.

2.4. Physical characterization

To perform the physical characterization of the electrocatalysts, two techniques were used. X-ray diffraction, to determine the crystalline structure of the material and Transmission electron microscopy, to determine the material's morphology, the size of the nanoparticles and their dispersion in the support. The equipment used was: X'Pert Pro® PW3042 / 10 in the range between $20° < 2\Theta < 80°$ ($K\alpha Cu = 1.54Å$, scanning speed $0.025° \ s^{-1}$) for analysis of XRD and JEOL JEM®-2100 at 200 kV to obtain the images in transmission mode (TEM) and dark field image in scan mode (STEM). The elementary composition was investigated by X-ray energy dispersion

Table 1. Masses of the compounds in syntheses

Compound	Synthesis with commercial CeO_2 (g)	Synthesis with CeO_2 nanowire (g)
$Ni(NO_3)_2.6H_2O$	0.2053	0.2038
Carbon	0.1283	0.1282
CeO_2	0.0326	0.0321
$NaBH_4$	0.1360	0.1348

spectroscopy (XEDS) using the STEM mode and an Oxford energy spectrometer (Xplore®).

2.5. Electrochemical experiments

Electrochemical analyses were performed in alkaline medium of 1 mol L^{-1} KOH and N_2 was purged for 5 minutes before each analysis. A three-electrode configuration cell was used for the electrochemical experiments. A Hg/HgO electrode and a platinum plate were used as the reference electrode and counter electrode, respectively. A glassy carbon (GC) with a geometric area of 0.196 cm^2 was used as the working electrode. The experiments were carried out using a DropSens® potentiostat.

From each synthesized catalyst, dispersions were prepared using 6 mg of catalyst, 300 µL of isopropyl alcohol, 700 µL of deionized water and 20 µL of nafion®. The dispersion was homogenized for 20 minutes on ultrasonic bath. 8 µL of the dispersion was deposited on the GC electrode and dried at 60 °C for 5 minutes.

The electrochemical characterization in support electrolyte (1 mol L^{-1} KOH) was performed by cyclic voltammetry (CV) measurements between 0 and 0.7 V *vs* Hg/HgO where 10 cycles were collected with a scanning speed of 10 mV s^{-1}. The electrocatalytic activity of the materials was evaluated in the presence of 1 mol L^{-1} KOH and 0.33 mol L^{-1} urea by CV between 0 and 0.7 V *vs* Hg/HgO where 5 cycles were collected with a scan rate of 10 mV s^{-1}. At last, chronoamperometry (CA) measurements were performed for 1 hour at 0.55 V in 0.33 mol L^{-1} urea and 1 mol L^{-1} KOH. The concentration of 0.33 mol L^{-1} was used to simulate the concentration of urea in human urine.[2] The normalization of the data was performed by the geometric area of the electrode.[16]

3. Results and Discussion

3.1. Physical characterization

The XRD patterns of the Ni/C, Ni/C-CeO_2 commercial and Ni/C-CeO_2 nanowire electrocatalysts are shown in Figure 1. In the XRD diffractogram of Ni/C material, it is possible to observe the peaks related to $Ni(OH)_2$ located in 2Θ = 33.5°; 38.6° and 59.7° attributed to the reflection plans {100}, {101} and {110},[24] respectively. The peaks for Ni° are also found at 2Θ = 44.7°; 52.0° and 76.6° corresponding to the crystalline planes {111}, {200} and {220},[16] respectively. The peak at 76.6° has a lower intensity among the three listed and was not observed, which may be related to the small size of the nanoparticles, as previously observed in the literature.[15,25] The peak located at 2Θ = 25.0° can be attributed to the reflection plane {002} of the graphite in Carbon Vulcan®.[11,26] Materials containing CeO_2 show peaks at 2Θ = 28.6°; 33.0°; 47.4°; 56.1°; 58.9°; 69.4°; 76.6° and 78.9° corresponding to the planes {111}, {200}, {220}, {311}, {222}, {400}, {311} and {420} of a face centered cubic structure of CeO_2.[27] The presence of $Ni(OH)_2$ in the Ni/C-CeO_2 nanowire material can

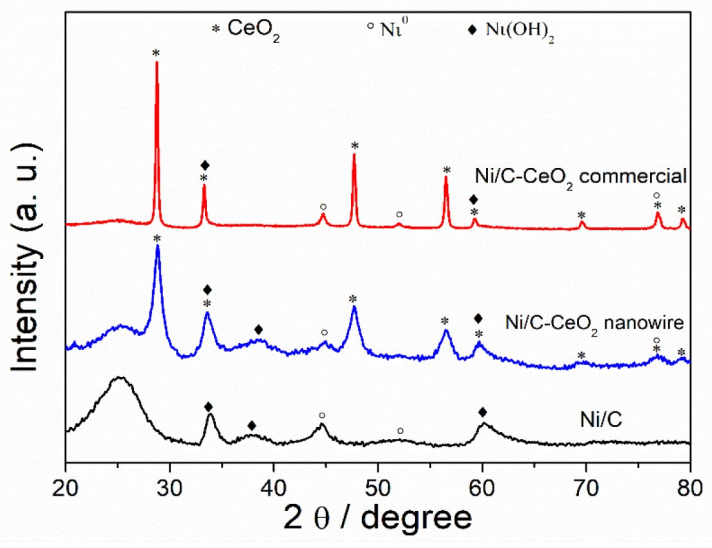

Figure 1. XRD patterns of Ni/C, Ni/C-CeO_2 commercial and Ni/C-CeO_2 nanowire electrocatalysts

be confirmed by the peak at 38.6° since the peaks at 33.5° and 59.7° attributed to this phase are very close to those of CeO_2 present in the support. It is also possible to observe that the peak attributed to Ni° at 44.7° is less intense, while the peak at 76.6° cannot be confirmed because it is at the same diffraction angle as CeO_2. The peak at 52.0° cannot be observed either because the nickel particles are very small.[25] It is possible to observe that all the diffraction peaks of the ceria nanowire are broader and in less intensity in relation to the commercial ceria, which may be related to the formation of smaller crystallites.[23] In the commercial Ni/C-CeO_2 diffractogram, except for the peak at 38.6°, all other peaks present in the material can be clearly seen.

Figure 2a shows an image obtained by transmission electron microscopy of Ni/C material. It is possible to observe the presence of nickel nanoparticles (in black, indicated by the arrow) with approximately 2 nm in diameter. Figure 2b shows the transmission electron microscopy image operating in scan mode (STEM). It was not possible to visualize the nickel nanoparticles by this technique, probably due to the small size of the particles. However, an important fact of STEM analyzes is the possibility to perform elemental mapping by XEDS, making it possible to obtain information about the dispersion of the different elements that make up the sample. In Figure 2c, in red, it is noted the presence of nickel superimposed on carbon in yellow. A uniform distribution of C and non-uniform Ni is observed, which is in higher concentration in the central region of the figure. In Figures 2 d-f, it is possible to analyze, individually, the mapping images of the elements nickel, oxygen and carbon, proving the dispersion of the elements in the material. In addition, it is observed the presence of oxygen in higher intensity over the region where nickel is present. This fact suggests the formation of some nickel and oxygen compounds, which corroborates with the presence of the peak referring to $Ni(OH)_2$ observed in the XRD patterns.

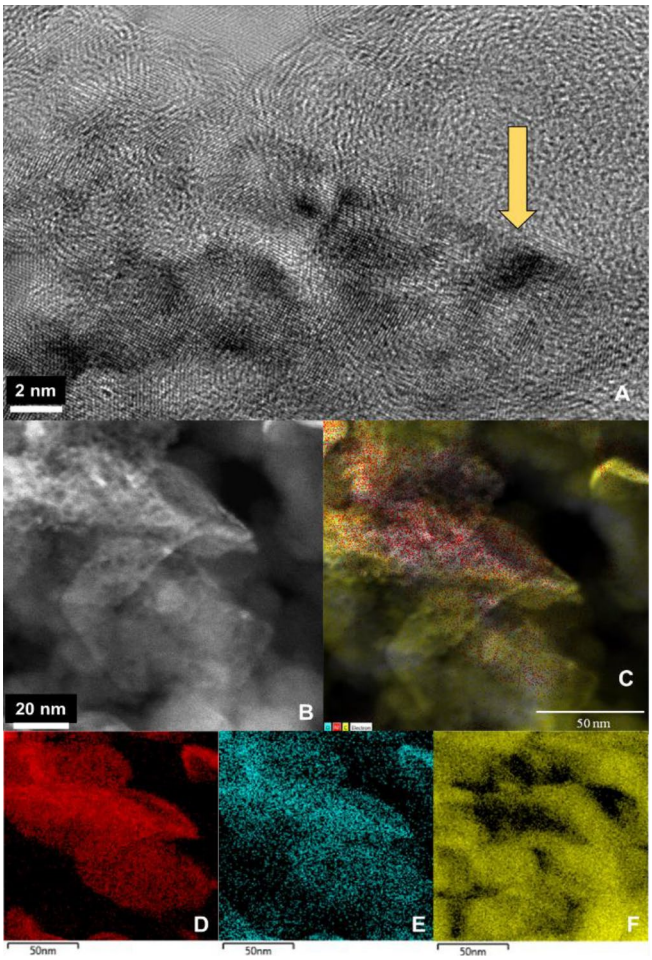

Figure 2. (a) Ni/C TEM (b) Ni/C STEM (c) Ni/C mapping (d) Ni mapping (e) O mapping (f) C mapping

The presence of nanowires with a diameter close to 15 nm can be confirmed from the TEM image shown in Figure 3a. In Figure 3b, it is possible to see an image with higher magnification of a single nanowire. In 3c, Ni/C-CeO_2 STEM image, the presence of ceria nanowires is indicated by arrows. In 3d-h, there are the XEDS mappings, where it is observed the Ni/C-CeO_2 mapping in 3d and each element individually in the other images. In Figure 3e, it is possible to define the region with the highest nickel concentration. Figure 3f shows the presence of ceria nanowires in the regions indicated in Figure 3c. In 3g, a higher oxygen intensity can be observed in the regions where nickel and cerium are present. The approximately uniform distribution of carbon over the entire surface area can be seen in Figure 3h. It is worth mentioning the simultaneous concentration of nickel and cerium in the same region, showing the interaction between these elements.

Figure 4a represents the STEM image of Ni/C-CeO_2 commercial catalyst. The XEDS mappings are at 4b-f. From Figure 4b, it is possible to see the overlapping of the signals referring to the different elements that make up the sample. In 4c, it is clear to notice how the nickel is dispersed throughout the material. In Figure 4d, the regions with the highest cerium concentration can be observed. By the analysis of this image, it is evident that the regions with the highest brightness in Fig. 4a refer to cerium. Also, there is no control of the morphology in the commercial ceria. Analyzing Figure 4e, it can be seen that oxygen is also dispersed in the regions with the highest concentration of nickel and cerium, evidencing the incorporation of oxygen in the crystalline network of the phases formed by these elements. Finally, in Figure 4f, there is an approximately uniform distribution of carbon in all material.

Therefore, with the results presented in Figures 2, 3 and 4, the presence of nickel in the materials

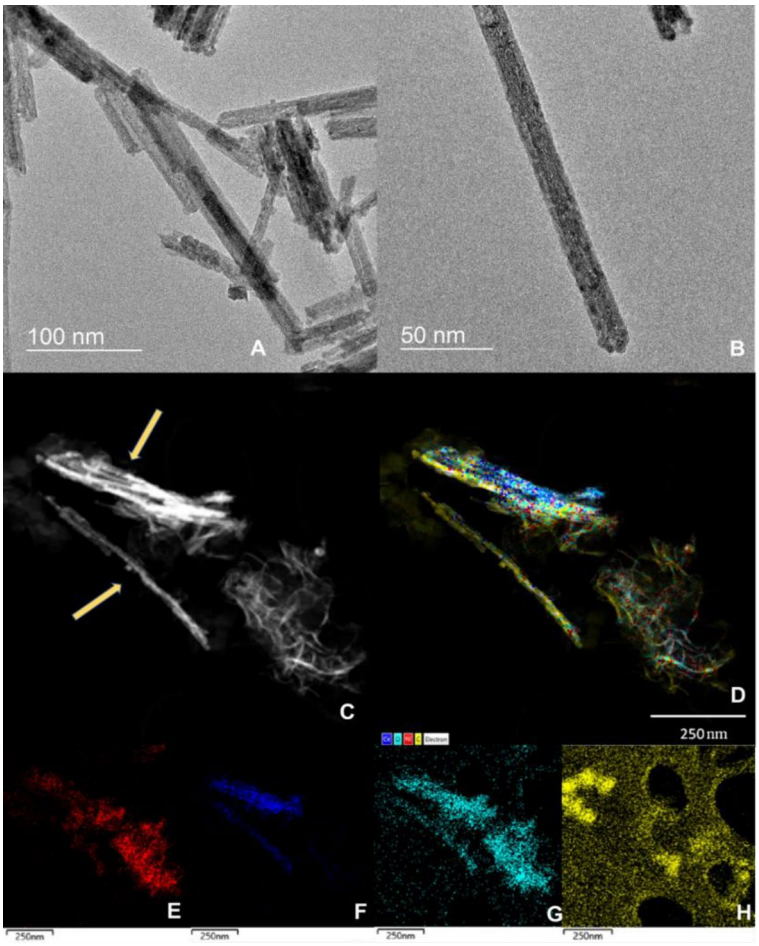

Figure 3. (a) CeO_2 nanowires (b) CeO_2 nanowires (c) Ni/C-CeO_2 nanowires (d) Ni/C-CeO_2 mapping (e) Ni mapping (f) Ce mapping (g) O mapping (h) C mapping

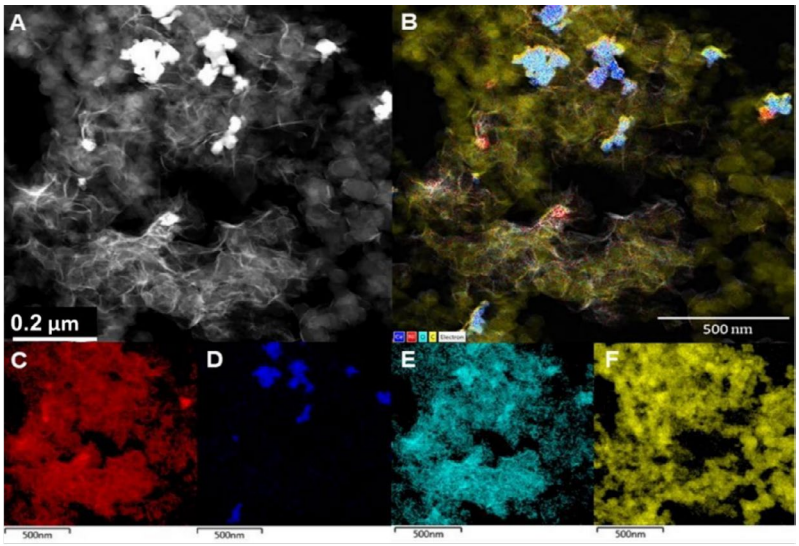

Figure 4. (a) Commercial Ni/C-CeO_2 STEM (b) Ni/C-CeO_2 commercial mapping (c) Ni mapping (d) Ce mapping (e) O mapping (f) C mapping

is explicit, as well as the presence of ceria in Ni/C-CeO_2 nanowire and Ni/C-CeO_2 commercial samples. The distribution of nickel and cerium in the catalysts obtained using XEDS mapping is in accordance with the distribution reported in the literature.[8]

3.2. Electrochemical experiments

Figure 5 shows the cyclic voltamograms of electrocatalysts synthesized in 1 mol L^{-1} KOH. The three cyclic voltamograms showed typical redox characteristics of Ni electrocatalysts.[28,29] For Ni/C electrocatalyst, two peaks can be observed. They are positioned at 0.51 V in the direct scan and 0.37 V in the reverse scan, where the peak in the direct scan refers to the oxidation of Ni^{2+} ($Ni(OH)_2$) to Ni^{3+} (NiOOH), while the peak of the reverse scan corresponds to the reduction of Ni^{3+} to Ni^{2+}.[4,24,30] For Ni/C-CeO_2 commercial and Ni/C-CeO_2 nanowire materials, the peaks in the direct scan were shifted to higher potential values, 0.53 and 0.54 V, respectively. While in the reverse scan, the peaks are shifted to lower potentials at 0.34 V and 0.33 V, for Ni/C-CeO_2 commercial and Ni/C-CeO_2 nanowire, respectively. Besides the variation in the values of the peak potentials, it is also noted that the presence of ceria causes a widening of them, a fact that has not been explained in the literature yet. However, it is evident that the presence of ceria causes a small change in the nickel voltamogram.

Figure 6 represents the cyclic voltammetry in 1 mol L^{-1} KOH and 0.33 mol L^{-1} urea. It shows a higher current density of the urea electro-oxidation process for the electrocatalyst Ni/C-CeO_2 nanowire. The maximum current density in the presence of Ni/C-CeO_2 nanowire was approximately 2.2 and 1.3 times higher than in the presence of Ni/C and Ni/C-CeO_2 commercial electrocatalysts, respectively. An important aspect that must be considered is that the urea oxidation process starts at approximately 0.45 V *vs* Hg/HgO, region of potential corresponding to the formation of NiOOH, which is the active phase to promote the urea electro-oxidation.[9] This fact is more expressive in materials containing CeO_2, revealing that the presence of ceria allows higher values of current density in the process of urea electro-oxidation in an alkaline medium.

It is important to highlight that the oxidation of urea depends on the regeneration of the catalyst surface, since the hydroxyl groups, important for the oxidation process, are obtained mostly from the NiOOH phase generated on the electrode surface during the activation stage.[16]

The presence of ceria in the urea electro-oxidation process is able to inhibit the deactivation of the NiOOH phase by the CO, an intermediate formed during the process. The oxygen storage capacity of ceria facilitates the oxidation of CO to CO_2, which is detached from the surface of the catalyst, avoiding the deactivation of the NiOOH phase and releasing active sites for urea molecules to oxidize.[8]

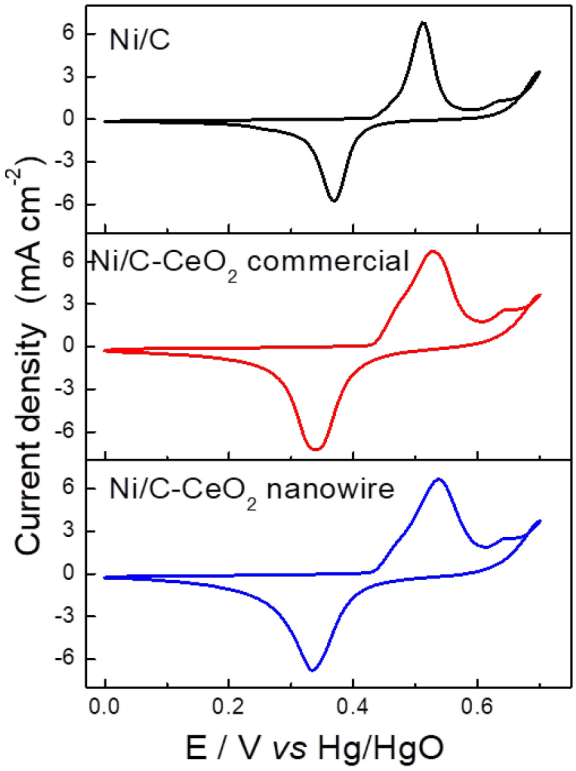

Figure 5. Cyclic voltammetry of the synthesized materials in 1 mol L^{-1} KOH and v = 10 mV s^{-1}

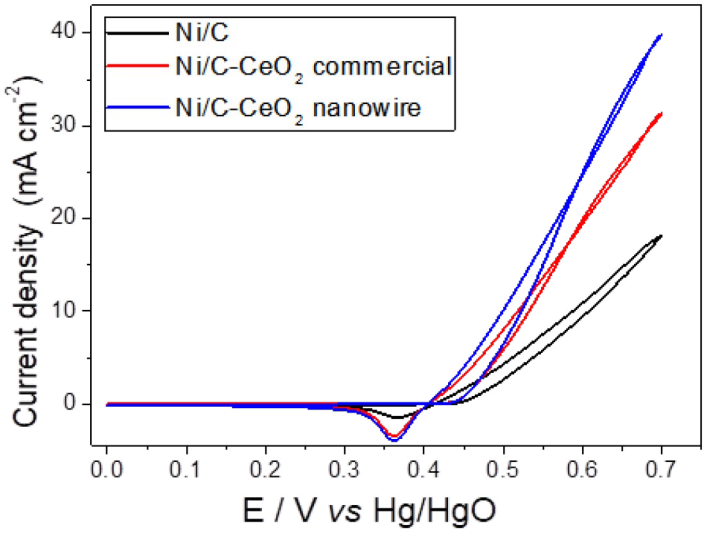

Figure 6. Cyclic voltammetry of the synthesized materials in 1 mol L^{-1} KOH and 0.33 mol L^{-1} of urea and v = 10 mV s^{-1}

Better results were obtained for the CeO_2 nanowires since this morphology has planes {110} and {100} preferably exposed on its surface, making CO oxidation more effective.[31] While in spherical nanoparticles, the exposed plane is preferably the {111} that store less oxygen, and consequently, less catalytic activity towards CO oxidation.[21]

Chronoamperometry measurements under a fixed potential of 0.55 V were performed for 60 minutes to analyze the catalytic stability of the nanomaterials towards the electro-oxidation reaction of urea, as shown in Figure 7. It is possible to notice a small fluctuation of the current signal during the analysis. It happens due to the release of gaseous products adsorbed on the catalyst

surface.[32] Because of this, a relatively low potential was chosen for the stability analysis. A decline in catalytic activity is noted, which may be related to the adsorption of intermediates such as CO on the surface of the catalysts.

The worst result in terms of current obtained from the urea electro-oxidation process was the one using Ni/C material, which proves again that the presence of ceria improves the catalytic activity in the case studied. Among the materials containing ceria, Ni/C-CeO_2 nanowire obtained a better result, a fact that is probably associated with the plans {110} and {100} preferably exposed in the ceria nanowires. It should be noted that, at the end of the process, the current density obtained with Ni/C-CeO_2 nanowire catalyst was 20% and 54% higher than that obtained with the Ni/C-CeO_2 commercial and Ni/C catalysts, respectively.

Therefore, it is evident, by the analysis of the results of cyclic voltammetry and chronoamperometry, that the addition of ceria to the carbon support, makes it possible to extract higher values of current density in the process of the urea electro-oxidation reaction. It has been reported in the literature that the addition of different metals to nickel catalysts, such as platinum,[15] molybdenum,[32] rhodium[29] and cobalt[3] also results in an enhancement of the catalytic activity toward electro-oxidation. In this sense, as it was mentioned previously, cerium is an abundant and cheap element, making it promising for the application reported in this study.

4. Conclusion

Ni/C, Ni/C-CeO_2 commercial and nanowire catalysts were successfully synthesized. From the XRD results, it is noted that the electrocatalysts are in the Ni° and $Ni(OH)_2$ phases and the characteristic peaks of CeO_2 and Vulcan® carbon are present. TEM images made it possible to confirm the morphology of the materials, to determine the diameter of the CeO_2 nanowires (approximately 15 nm) and the size of the nickel nanoparticles (approximately 2 nm) and the distribution of the elements that make up the materials. The CV experiments revealed that the addition of nanowire ceria in the support caused an increase of about 30% in the maximum current density in relation to the addition of commercial ceria and 120% in relation to nickel supported only on carbon. In the CA experiments, the current density at the end of the process using the Ni/C-CeO_2 nanowire catalyst was 20% higher than the one obtained over Ni/C-CeO_2 commercial and 54% than the one obtained with Ni/C.

The best results obtained with materials containing ceria may be related to the oxygen supply, since it has a remarkable oxygen storage capacity with great mobility within the crystalline structure due to the presence of the Ce^{3+}/Ce^{4+} pair, facilitating the oxidation of reaction intermediates. The presence of ceria nanowires was more significant probably due to the planes {110} and

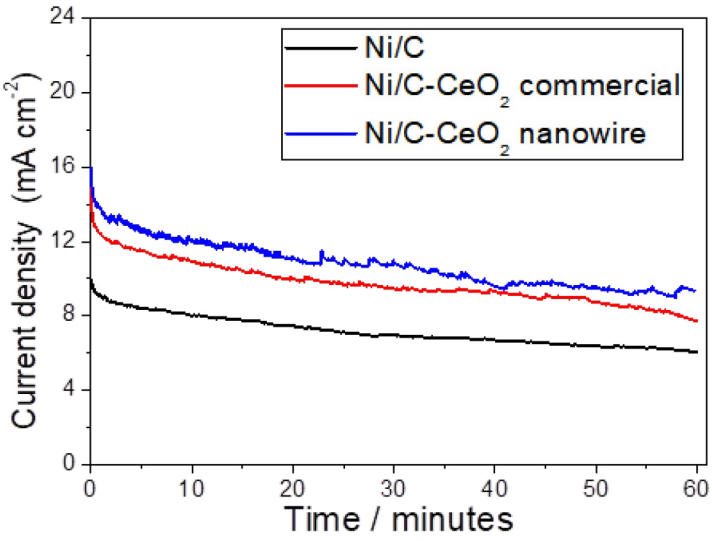

Figure 7. Chronoamperometry of the synthesized materials in 1 mol L^{-1} KOH and 0.33 mol L^{-1} of urea at 0.55 V for 60 minutes

{100} preferably exposed on its surface, which are more effective in promoting CO oxidation than the planes {111} present in greater abundance in ceria nanoparticles.

Thus, Ni/C-CeO_2 nanowire material is a promising catalyst for the urea electro-oxidation reaction which could be used for removal of this compound in the wastewater treatment.

Acknowledgements

The authors would like to thank the scholarships and financial assistance from FAPERJ (Research Support Foundation of the State of Rio de Janeiro) process E-26/211371/2019, E-26/201.035/2019 and E-26/200153/2020, CNPq (National Council for Scientific and Technological Development) process 422614 / 2018-1, CAPES (Coordination for the Improvement of Higher Education Personnel). To CBPF (Brazilian Center for Physical Research) for the assistance with the equipment (XRD and TEM) to carry out the characterization analyzes of this work, to LABNANO-CBPF for the analyzes under the JEOL JEM-2100F microscope. This work was carried out with the support of the Coordination for the Improvement of Higher Education Personnel - Brazil (CAPES) - Financing Code 001.

References

[1] Rahimpour, M. R.; Barmaki, M. M.; Mottaghi, H. R. A comparative study for simultaneous removal of urea, ammonia and carbon dioxide from industrial wastewater using a thermal hydrolyser. *Chemical Engineering Journal* **2010**, *164*, 155. [CrossRef]

[2] Yan, W.; Wang, D.; Botte, G. G. Electrochemical decomposition of urea with Ni-based catalysts. *Applied Catalysis B: Environmental* **2012**, *127*, 221. [CrossRef]

[3] Yan, W.; Wang, D.; Botte, G. G. Nickel and cobalt bimetallic hydroxide catalysts for urea electro-oxidation. *Electrochimica Acta* **2012**, *61*, 25. [CrossRef]

[4] Vedharathinam, V.; Botte, G. G. Understanding the electro-catalytic oxidation mechanism of urea on nickel electrodes in alkaline medium. *Electrochimica Acta* **2012**, *81*, 292. [CrossRef]

[5] Felix, E. P.; Cardoso, A. A. Amônia (NH_3) atmosférica: Fontes, transformação, sorvedouros e métodos de análise. *Química Nova* **2004**, *27*, 123. [CrossRef]

[6] Vedharathinam, V.; Botte, G. G. Direct evidence of the mechanism for the electro-oxidation of urea on $Ni(OH)_2$ catalyst in alkaline medium. *Electrochimica Acta* **2013**, *108*, 660. [CrossRef]

[7] Boggs, B. K.; King, R. L.; Botte, G. G. Urea electrolysis: Direct hydrogen production from urine. *Chemical Communications* **2009**, *32*, 4859. [CrossRef]

[8] Tran, T. Q. N.; Yoon, S. W.; Park, B. J.; Yoon, H. H. CeO_2-modified $LaNi_{0.6}Fe_{0.4}O_3$ perovskite and MWCNT nanocomposite for electrocatalytic oxidation and detection of urea. *Journal of Electroanalytical Chemistry* **2018**, *818*, 76. [CrossRef]

[9] Yan, W.; Wang, D.; Diaz, L. A.; Botte, G. G. Nickel nanowires as effective catalysts for urea electro-oxidation. *Electrochimica Acta* **2014**, *134*, 266. [CrossRef]

[10] Baranova, E. A.; Cally, A.; Allagui, A.; Ntais, S.; Wüthrich, R. Nickel particles with increased catalytic activity towards hydrogen evolution reaction. *Comptes Rendus Chimie* **2013**, *16*, 28. [CrossRef]

[11] Silva, J. C. M.; Piasentin, R. M.; Spinacé, E. V.; Neto, A. O.; Baranova, E. A. The effect of antimony-tin and indium-tin oxide supports on the catalytic activity of Pt nanoparticles for ammonia electro-oxidation. *Materials Chemistry and Physics* **2016**, *180*, 97. [CrossRef]

[12] Silva, R. N.; Pocrifka, L. A.; Passos, R. R. Obtaining SnO_2@Pt/C, Ni@Pt/C and NiSn@Pt/C for application in the electrocatalyst of oxygen reduction reaction. *Revista Virtual de Química* **2019**, *11*, 1920. [CrossRef]

[13] Granja, D. S. S.; Da Silva, L. M. S.; Rodrigues, I. A. Nanomaterials applied as electrocatalysts in the oxidation reaction of ethanol. *Revista Virtual de Química* **2015**, *7*, 1635. [CrossRef]

[14] Sayed, E. T.; Eisa, T.; Mohamed, H. O.; Abdelkareem, M. A.; Allagui, A.; Alawadhi, H.; Chae, K. J. Direct urea fuel cells: Challenges and opportunities. *Journal of Power Sources* **2019**, *417*, 159. [CrossRef]

[15] Barbosa, J. R.; Paranhos, C. H.; Alves, O. C.; Checca, N. R.; Serna, J. P.; Rossi, A. L.; Silva, J. C. M. Low loading platinum dispersed on Ni/C nanoparticles as high active catalysts for urea electrooxidation reaction. *Electrochimica Acta* **2020**, *355*, 136752. [CrossRef]

[16] Barakat, N. A. M.; Motlak, M.; Ghouri, Z. K.; Yasin, A. S.; El-Newehy, M. H.; Al-Deyab, S. S. Nickel nanoparticles-decorated graphene as highly effective and stable electrocatalyst for urea electrooxidation. *Journal of Molecular Catalysis A: Chemical* **2016**, *421*, 83. [CrossRef]

[17]Campbell, C. T.; Peden, C. H. F. Oxygen vacancies and catalysis on ceria surfaces. *Science* **2005**, *309*, 713. [CrossRef]
[18]Abd El-Lateef, H. M.; Almulhim, N. F.; Mohamed, I. M. A. Physicochemical and electrochemical investigations of an electrodeposited $CeNi_2$@NiO nanomaterial as a novel anode electrocatalyst material for urea oxidation in alkaline media. *Journal of Molecular Liquids* **2020**, *297*, 111737. [CrossRef]
[19]Liu, X.; Zhou, K.; Wang, L.; Wang, B.; Li, Y. Oxygen vacancy clusters promoting reducibility and activity of ceria nanorods. *Journal of the American Chemical Society* **2009**, *131*, 3140. [CrossRef]
[20]Du, H.; Wang, Y.; Arandiyan, H.; Younis, A.; Scott, J.; Qu, B.; Wan, T.; Lin, X.; Chen, J.; Chu, D. Design and synthesis of CeO_2 nanowire/MnO_2 nanosheet heterogeneous structure for enhanced catalytic properties. *Materials Today Communications* **2017**, *11*, 103. [CrossRef]
[21]Tana; Zhang, M.; Li, J.; Li, H.; Li, Y.; Shen, W. Morphology-dependent redox and catalytic properties of CeO2 nanostructures: Nanowires, nanorods and nanoparticles. *Catalysis Today* **2010**, *148*, 179. [CrossRef]
[22]King, R. L.; Botte, G. G. Hydrogen production via urea electrolysis using a gel electrolyte. *Journal of Power Sources* **2011**, *196*, 2773. [CrossRef]
[23]Silva, A. G. M.; Batalha, D. C.; Rodrigues, T. S.; Candido, E. G.; Luz, S. C.; Freitas, I. C.; Fonseca, F. C.; Oliveira, D. C.; Taylor, J. G.; Torresi, S. I. C.; Camargo, P. H. C.; Fajardo, H. V. Sub-15 nm CeO_2 nanowires as an efficient non-noble metal catalyst in the room-temperature oxidation of aniline. *Catalysis Science and Technology* **2018**, *8*, 1828. [CrossRef]
[24]Zhou, X. C.; Yang, X. Y.; Fu, Z. B.; Yang, Q.; Yang, X.; Tang, Y. J.; Wang, C. Y.; Yi, Y. Single-crystalline ultrathin nanofilms of Ni aerogel with $Ni(OH)_2$ hybrid nanoparticles towards enhanced catalytic performance for ethanol electro-oxidation. *Applied Surface Science* **2019**, *492*, 756. [CrossRef]
[25]Chen, J.; Lu, Z. H.; Huang, W.; Kang, Z.; Chen, X. Galvanic replacement synthesis of NiPt/graphene as highly efficient catalysts for hydrogen release from hydrazine and hydrazine borane. *Journal of Alloys and Compounds* **2017**, *695*, 3036. [CrossRef]
[26]Barbosa, J. R.; Leon, M. N.; Fernandes, C. M.; Antoniassi, R. M.; Alves, O. C.; Ponzio, E. A.; Silva, J. C. M. $PtSnO_2$/C and Pt/C with preferential (100) orientation: High active electrocatalysts for ammonia electro-oxidation reaction. *Applied Catalysis B: Environmental* **2020**, *264*. [CrossRef]
[27]Zhou, G.; Gui, B.; Xie, H.; Yang, F.; Chen, Y.; Chen, S.; Zheng, X. Influence of CeO_2 morphology on the catalytic oxidation of ethanol in air. *Journal of Industrial and Engineering Chemistry* **2014**, *20*, 160. [CrossRef]
[28]Singh, R. K.; Schechter, A. Electrochemical investigation of urea oxidation reaction on β $Ni(OH)_2$ and $Ni/Ni(OH)_2$. *Electrochimica Acta* **2018**, *278*, 405. [CrossRef]
[29]Mirzaei, P.; Bastide, S.; Dassy, A.; Bensimon, R.; Bourgon, J.; Aghajani, A.; Zlotea, C.; Muller-Bouvet, D.; Cachet-Vivier, C. Electrochemical oxidation of urea on nickel-rhodium nanoparticles/carbon composites. *Electrochimica Acta* **2019**, *297*, 715. [CrossRef]
[30]Zhan, S.; Zhou, Z.; Liu, M.; Jiao, Y.; Wang, H. 3D NiO nanowalls grown on Ni foam for highly efficient electro-oxidation of urea. *Catalysis Today* **2019**, *327*, 398. [CrossRef]
[31]Phuruangrat, A.; Thongtem, S.; Thongtem, T. Microwave-assisted hydrothermal synthesis and characterization of CeO_2 nanowires for using as a photocatalytic material. *Materials Letters* **2017**, *196*, 61. [CrossRef]
[32]Yang, D.; Yang, L.; Zhong, L.; Yu, X.; Feng, L. Urea electro-oxidation efficiently catalyzed by nickel-molybdenum oxide nanorods. *Electrochimica Acta* **2019**, *295*, 524. [CrossRef]